

A Parallel Optical Image Security System with Cascaded Phase-only Masks

Shuming Jiao, Yang Gao, Ting Lei, Zhenwei Xie, Xiaocong Yuan*
Nanophotonics Research Centre, College of Optoelectronic Engineering, Shenzhen University,
Shenzhen, Guangdong, China
xcyuan@szu.edu.cn

Abstract—In many previous works, a cascaded phase-only mask (or phase-only hologram) architecture is designed for optical image encryption and watermarking. However, one such system usually cannot process multiple pairs of host images and hidden images in parallel. In our proposed scheme, multiple host images can be simultaneously input to the system and each corresponding output hidden image will be displayed in a non-overlap sub-region in the output imaging plane. Each input host image undergoes a different optical transform in an independent channel within the same system. The multiple cascaded phase masks (up to 25 layers or even more) in the system can be effectively optimized by a wavefront matching algorithm.

Index Terms—multiple, multiplexing, optical encryption, image hiding, phase-only mask

1. Introduction

Information security is a very critical issue in the acquisition, transmission and processing of various types of data such as images. In addition to the commonly used digital security technologies [1] solely based on computer algorithms, the research of optical image encryption, authentication and watermarking techniques [2-5] has received increasingly more attention in recent years. Optical security techniques exhibit certain potential advantages over digital techniques such as high parallelism, high processing speed and direct processing of physical objects.

One common optical architecture for image encryption and watermarking is the cascaded phase-only mask architecture [6-13], which can be dated back to the early work of Double Random Phase Encoding [6] two decades ago. Multiple cascaded phase-only masks (or referred to as phase-only holograms) are aligned at certain separation intervals either in a lens system (such as [6]) or a lensless system (such as [7]). Under coherent light illumination, the diffractive field of the input image is modulated by each phase-only mask sequentially during the forward propagation. Finally, the imaging result in the output plane is recorded as the ciphertext or retrieved hidden image. In many systems (such as [11-13]), the phase-only masks need to be appropriately designed to ensure the system output result is the target one.

In fact, as an optical information processing system, the cascaded phase-only mask architecture has been employed for optical mode conversion [14-16] and optical pattern recognition [17] in previous works, in addition to optical image security. In the work [17], a deep learning network is implemented all optically with a cascaded phase-only mask architecture. The phase-only masks in these systems are usually designed by certain optimization algorithms such as Gerchberg–Saxton iteration [11-13], wavefront matching [16] and error back-propagation [17].

In optical security, a cascaded phase mask system can be employed as an encryption system [6-10], which transforms an original image into a noise-like ciphertext. The multiple phase-only masks can be used as the encryption and decryption keys. Unauthorized users without knowing the key cannot recover the original image from the ciphertext. Moreover, a cascaded phase mask system can be employed as an image hiding system [11-13]. The host image is input to the system and another hidden image will be displayed at the output imaging plane, which is a natural image completely different from the input one. Unauthorized users will not be able to disclose the hidden image from the host image without a set of correct phase masks.

Conventionally, one such optical security system [6-13] with a given set of phase-only masks can only perform encryption or image hiding for a specific pair of input-output images at one time. To overcome this limitation, the encryption or hiding of multiple images using the same optical architecture has been extensively investigated [18-22]. However, in these works [18-22], the system usually only performs a transformation from multiple input images to one single output and the output signals from each individual input are mixed. In this work, we propose a novel multiplexing system to perform a transformation from multiple input images to multiple output images in a parallel manner, which was seldom investigated previously in optical security field. To certain extent, this work can be considered as a generalization of the previous work [13].

In our work, the processing of each different input-output image pair can be considered as an independent “channel”, which can be favorable in many practical applications. For example, in some previous works [23-26], optical security systems are designed for biometric authentication such as face recognition and fingerprint verification. The system can display the password image to the user if the user’s biometric feature is successfully authenticated. However, one system may be only used for the verification of one specific user. As a significant advantage, our proposed system can support the verification for multiple users and display

different output message to each individual user in a parallel manner.

This paper is organized as follows. The working principles of our proposed system will be described in Section 2. The simulation results and discussions will be given in Section 3. A brief conclusion will be made in Section 4.

2. Proposed Parallel Optical Image Security System with Cascaded Phase Masks

A. General Framework of Our Proposed System

In our proposed scheme, multiple host images, with each being multiplied by a different phase mask, can be simultaneously input to the system. Under coherent light illumination, the superposed diffractive field will propagate and pass through multiple phase-only masks sequentially. Finally, multiple hidden images will be displayed in non-overlap sub-windows in the output imaging plane. The transformation of each input host image to its corresponding output hidden image is performed in an independent channel with the same set of cascaded phase masks.

A general framework of our proposed system is illustrated in Fig.1. It is assumed that our proposed scheme is designed to simultaneously transform K input host images I_1, I_2, \dots, I_{K-1} and I_K into K output hidden images O_1, O_2, \dots, O_{K-1} and O_K . The size (number of pixels) of the output imaging plane and that of each input host image are identical. In our proposed system, a different random phase-only mask is placed in each input port (at the position of the input imaging plane) and there are totally K different random phase masks. The random phase masks R_1, R_2, \dots, R_{K-1} and R_K can be arbitrarily generated as long as they are random and different from each other. The reason why each input image is modulated by a different random phase mask first can be explained as follows. After the multiplication with random phase masks, $I_1 R_1, I_2 R_2, \dots, I_K R_K$ will become approximately orthogonal to each other, which means the inner product between any two of them (e.g. between $I_1 R_1$ and $I_3 R_3$) will be approximately zero. It shall be noted that the phase masks multiplied with each host image have to be random and different from each other. If the masks are the same for different images, the orthogonality cannot be achieved. In a cascaded phase-only mask system, orthogonal inputs and orthogonal outputs are favorable for parallel processing, as discussed in [27].

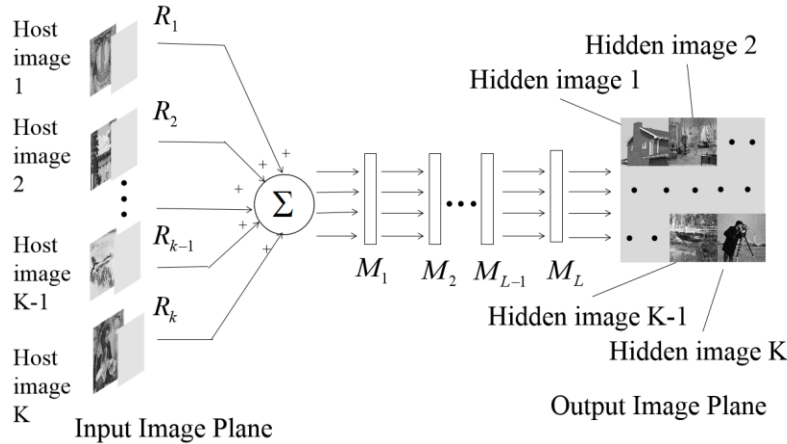


Fig. 1. Architecture of our proposed parallel optical image hiding system (R denotes each random phase mask and M denotes each optimized cascaded phase-only mask).

Then each input image modulated by its corresponding phase mask is illuminated by a coherent plane wave with the same wavelength. All the diffractive fields will be superposed and propagate from the input imaging plane to the first optimized phase mask M_1 . The superposition of light fields can be optically implemented with beam combiners, like the superposition of object wave and reference wave in holography. It is assumed the system consists of totally L optimized phase masks ($M_1, M_2, \dots, M_{L-1}, M_L$) and for simplicity the neighboring masks are all placed at a distance interval of d . In addition, the distance between the input imaging plane and the mask M_1 and the distance between the output imaging plane and the mask M_L are assumed to be d as well. It shall be noticed that the interval distances between masks can be flexibly adjusted and not necessarily all equal. The superposed diffractive field will propagate and pass through each optimized phase mask sequentially. Finally, the light intensity of the diffractive field at the output imaging plane will be recorded. The output imaging plane is divided into K regions and in each region the retrieved hidden image for each corresponding input image will be displayed. The K hidden images are non-overlap and each occupies at most $1/K$ area. In other words, the size (number of pixels) of each individual output image is at most $1/K$ of the input image if the input imaging plane and output imaging plane have identical size. The non-overlapped windows for displaying each output image are orthogonal to each other since they are spatially separate [27].

The most important feature of our proposed system is that the processing of each pair of input-output images is independent. The system can accept all the K input host images simultaneously, or only accept one single input host image, or accept an arbitrary

subset of all the input host images. The corresponding output images will be displayed in the pre-designed regions of the output imaging plane and the “deactivated” regions will be blank.

One critical issue in our proposed scheme is how to design the L optimized phase-only masks to ensure that the system can yield the desired output imaging results. In our work, a wavefront matching algorithm [16] is employed to optimize the phase values of each pixel in the phase-only masks. This algorithm is different from the commonly used Gerchberg–Saxton algorithm [11-13, 18-22] in previous relevant works.

B. Wavefront Matching Algorithm for Designing the Optimized Phase-only Masks

The wavefront matching algorithm for designing the optimized phase masks in our proposed system is described as follows. A simple system only consisting of two phase-only masks M_1 and M_2 is taken as an example for explanation. For simplicity, it is assumed that the system is designed for multiplexing two pairs of host images and hidden images (I_1 and O_1 , I_2 and O_2 , shown in Fig. 2). The number of phase masks and the number of image pairs can be far more than two. But the working principles remain the same.

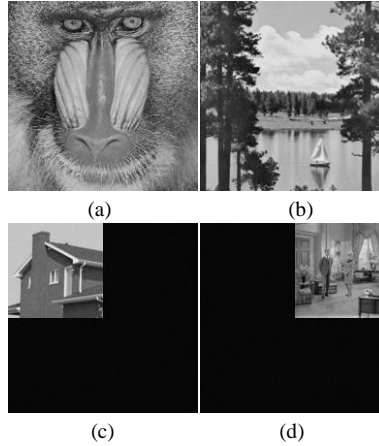


Fig. 2. Two pairs of input images and output images for parallel image hiding (a) Input host image I_1 ; (b) Input host image I_2 ; (c) Output hidden image O_1 ; (d) Output hidden image O_2 .

As stated above, the two host images I_1 and I_2 , multiplied with corresponding phase masks R_1 and R_2 , can be simultaneously input to the system as $(I_1 R_1 + I_2 R_2)$ or each one can be individually input to the system, shown in Fig. 3. The intensity of the output field will vary according to the actual input but the output phase plane is assumed to be invariant as P , which is an extra constraint condition in the optimization.

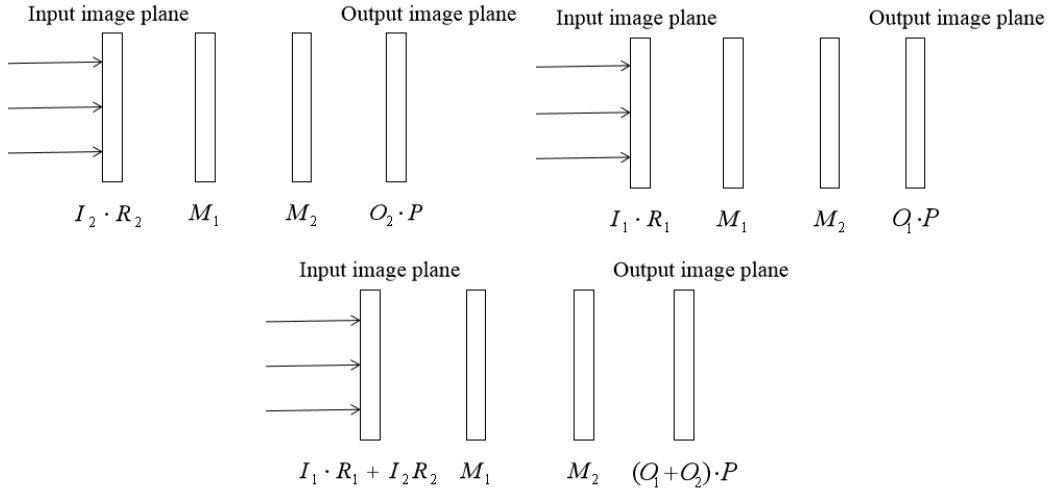


Fig. 3. A simple example of proposed system with only two layers of optimized phase-only masks. The system can multiplex two input-output image pairs and the input can (a) only include image I_1 and corresponding random phase mask R_1 ; (b) only include image I_2 and corresponding random phase mask R_2 ; (c) include both.

The optimization of phase-only masks is implemented iteratively. In each iteration, there will be three steps ($L+1$ steps if there are L cascaded phase masks in the system). Initially, M_1 , M_2 and P are set to be random phase masks. They will be updated in

each iteration whereas R_1 and R_2 are unchanged.

Step One: the input field propagates forward to the back of M_1 and the output field propagates backward to the front of M_1 . Each input host image and output hidden image is processed individually illustrated in (1)-(4), with $f(\dots, d)$ representing a free-space Fresnel field propagation with distance d (either forward propagation with a positive value or backward propagation with a negative value). The phase mask M_1 is updated according to the rules in (5), with $\text{Phase}[\dots]$ representing the retrieval of phase part.

$$D_{\text{forward}1} = f(I_1 R_1, d); \quad (1)$$

$$D_{\text{forward}2} = f(I_2 R_2, d); \quad (2)$$

$$D_{\text{back}1} = f[f(O_1 P, -d) / M_2, -d]; \quad (3)$$

$$D_{\text{back}2} = f[f(O_2 P, -d) / M_2, -d]; \quad (4)$$

$$M_1 = \text{Phase}[D_{\text{back}1} / D_{\text{forward}1} + D_{\text{back}2} / D_{\text{forward}2}]; \quad (5)$$

Step Two: similar to Step One, the input field propagates forward to the back of M_2 and the output field propagates backward to the front of M_2 . The phase mask M_2 is updated according to (6), as:

$$M_2 = \text{Phase}[f(O_1 P, -d) / f(f(I_1 R_1, d) M_1, d) + f(O_2 P, -d) / f(f(I_2 R_2, d) M_1, d)]; \quad (6)$$

Step Three: the input field propagates forward to the output plane and the constant output phase P is updated according to (7), as:

$$P = \text{Phase}[f(f(f(I_1 R_1, d) M_1, d) M_2, d) + f(f(f(I_1 R_1, d) M_1, d) M_2, d)]; \quad (7)$$

After Step Three, the algorithm will enter the next iteration and starts with Step One again. After a certain number of iterations, the algorithm will finally converge and the optimized phase-only masks M_1 and M_2 are finally obtained. The wavefront matching algorithm for phase mask optimization is illustrated in Fig. 4.

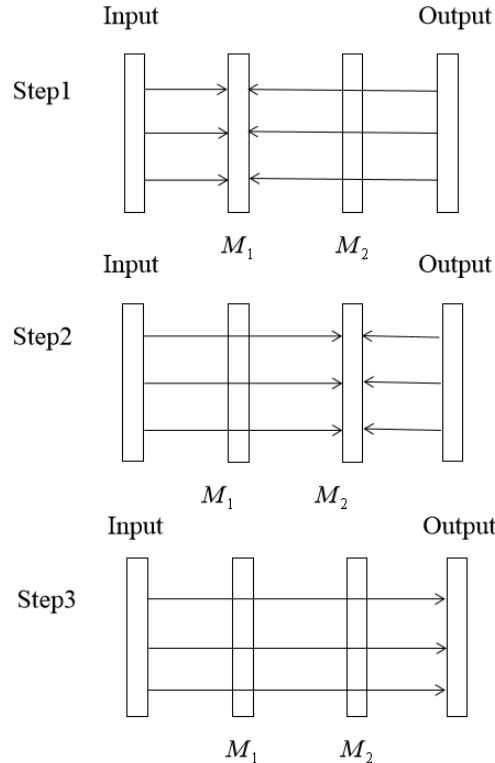


Fig. 4. Wavefront matching algorithm for phase mask optimization in our proposed system

3. Result and Discussion

In the simulation, four input-output image pairs are tested with our proposed parallel optical image hiding system consisting of six cascaded optimized phase-only masks. The horizontal and vertical extent of each input image (host image) is 512×512 pixels. The horizontal and vertical extent of each output image (hidden image) is 256×256 pixels. The pixel size is $8 \mu\text{m}$ and the separation distance d is 0.05m . The wavelength of the illumination light is 632nm . Four pairs of pre-defined input host images and output

hidden images are shown in Fig. 5 and Fig. 6 respectively.

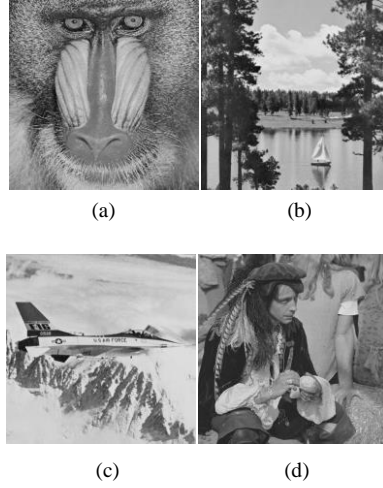


Fig. 5. Four pre-defined input host images in the optical image hiding systems: (a) Input host image I_1 ; (b) Input host image I_2 ; (c) Input host image I_3 ; (d) Input host image I_4 .

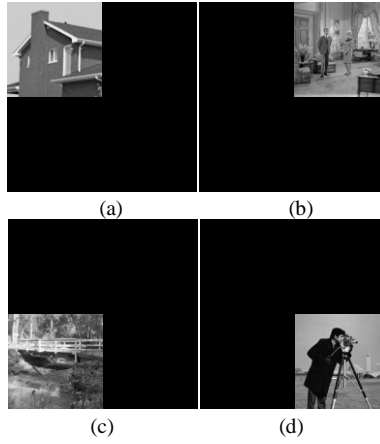
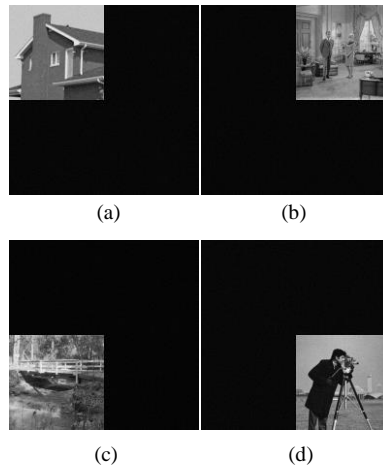


Fig. 6. Four pre-defined output hidden images in the optical image hiding systems (a) Corresponding to Fig 5(a); (b) Corresponding to Fig 5(b); (c) Corresponding to Fig 5(c); (d) Corresponding to Fig 5(d).

After 30 iterations of optimization using wavefront matching algorithm, the optimized phase masks can be obtained. The output imaging results are shown in Fig. 7 when the system input is set to be varying host images.



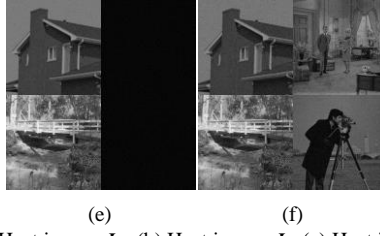


Fig. 7. System output results when the system input is (a) Host image I_1 ; (b) Host image I_2 ; (c) Host image I_3 ; (d) Host image I_4 ; (e) Host image I_1 plus Host image I_3 ; (f) All host images.

It can be observed that the designed system can correctly display the desired hidden images in the corresponding regions of the output imaging plane. When a subset of input images is fed into the system, only the corresponding output images will be displayed and the remaining regions are blank. An acceptable level of noise can be observed in the results. The noise problem in optical security systems can be possibly solved by error correction coding [28, 29].

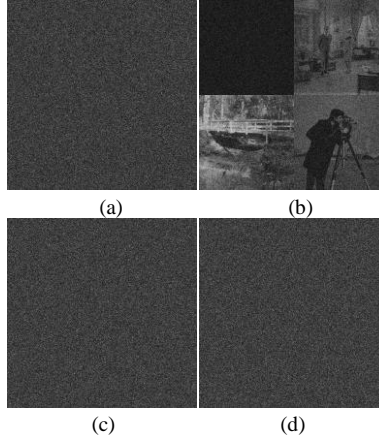


Fig. 8. (a) System output result when the input is host image I_1 with wrong R_1 mask; (b) System output result when the input includes all the four host images with wrong R_1 mask and correct R_2 , R_3 and R_4 masks; (c) System output result when the input is host image I_1 with wrong M_1 mask; (d) System output result when the input includes all the four host images with wrong M_1 mask.

The four random phase masks (R_1, R_2, R_3 and R_4) and six optimized cascaded phase masks (M_1, M_2, M_3, M_4, M_5 and M_6) can be employed as security keys. The desired output images can only be displayed when the input image multiplied with corresponding random phase mask is correct and all the cascaded phase mask keys are correct. Otherwise, only random-noise results will be obtained in the output imaging plane, shown in Fig.8.

The number of optimized phase-only masks in the system, L , is not limited to four and can be theoretically increased to infinity. As the number of phase mask layers increases, the quality of the output imaging results will be enhanced if the number of input-output image pairs remain fixed, shown in Fig. 9. The SSIM (Structural Similarity Index) image quality indices for Fig. 9(a), Fig. 9(b) and Fig. 9(c) compared with original reference images are 0.3986, 0.6684 and 0.8655 respectively, as the number of layers increases from 4 to 6 and 10. The reason is that an increased number of phase-only masks can bring more degrees of freedom in the optical transforms. The mapping function between input images and output images will be simulated more accurately by the optical system.





(b)



(c)

Fig. 9. Output imaging result when all the four host images are input to the system: (a) 4 layer of phase masks ($L=4$); (b) 6 layers of phase masks ($L=6$); (c) 8 layers of phase masks ($L=8$).

In addition, the amount of noise in the output imaging results will generally increase when the number of parallel input-output image pairs K increases if the number of phase mask layer is fixed, shown in Fig. 10. The SSIM image quality indices for Fig.10(a), Fig.10(b) and Fig.10(c) compared with original reference images are 0.7307, 0.4963 and 0.3986 respectively, as the number of parallelly processed image pairs increase from 2 to 3 and 4.



(a)



(b)



(c)

Fig. 10. Output imaging result when the system contains 4 layers of phase masks ($L=4$) and all of K host images are input: (a) $K=2$; (b) $K=3$; (c) $K=4$.

It can be inferred from the results above that an increasing number of cascaded phase-only masks in the system allows the multiplexing of more image pairs without loss of output imaging quality. In other words, a higher information processing capacity of our proposed system can be achieved if the number L is increased. In Fig. 11, the optical image hiding for 16 pairs of input and output images can be realized with a system consisting of 15 layers or 25 layers of phase masks, with better output imaging quality in the latter architecture. The 16 input host images can be transformed into 16 output hidden images (different from any host image) in a parallel manner. An open source Matlab code for the simulation of our proposed system can be found in [30].



(a)



(b)

(c)

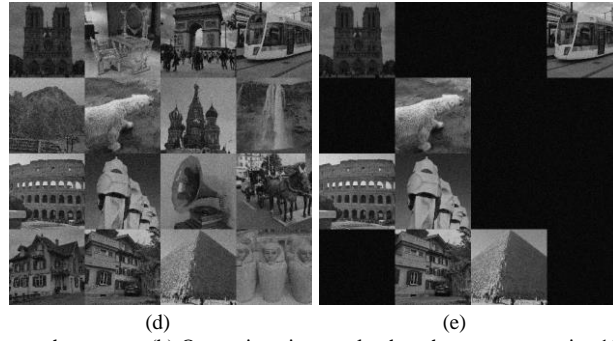


Fig. 11. (a) 16 different input host images input to the system; (b) Output imaging result when the system contains 15 layers of phase masks ($L=15$) and all of 16 host images are used as the input; (c) Output imaging result when the system contains 15 layers of phase masks ($L=15$) and a subset of the host images are used as the input; (d) Output imaging result when the system contains 25 layers of phase masks ($L=25$) and all of 16 host images are used as the input; (e) Output imaging result when the system contains 25 layers of phase masks ($L=25$) and a subset of the host images are used as the input.

4. Conclusion

An optical architecture with cascaded phase-only masks (or phase-only holograms) is often employed for optical information processing such as optical mode conversion, optical deep learning and optical security. In previous works, such an architecture is attempted for transforming one single input image to one single output image, or multiple input images into one single output, for encryption or watermarking. In this work, we propose a parallel optical image hiding system that can process multiple pairs of input-output images in a parallel manner for the first time.

Each input host image is multiplied with a random phase mask first and the complex light field can be individually or jointly input to a cascaded phase-only mask architecture with L layers. With the propagating diffractive field being modulated by each phase mask sequentially, the desired output results will be displayed in each spatially separated sub-windows of the output imaging plane.

In this work, a wavefront matching algorithm is employed to optimize the L phase masks in the system, different from the commonly used Gerchberg–Saxton algorithm. The algorithm can be used to design a cascaded phase mask system with many layers (e.g. more than 20). As a contrast, in previous optical security works (such as [2-13]), the number of layers is usually restricted to two to four layers.

Simulation results reveal that our proposed system can achieve good imaging quality, low cross-talk between different channels and good security for image hiding.

Reference

- [1] B. Furht, E. Muharemagic, and D. Socek, "Multimedia encryption and watermarking," Springer Science and Business Media, 2006.
- [2] B. Javidil, A. Carnicer, M. Yamaguchi, T. Nomura, E. Pérez-Cabré, M. S. Millán, N. K. Nishchal, R. Torroba, J. F. Barrera, W. Q. He, X. Peng, A. Stern, Y. Rivenson, A. Alfalou, C. Brosseau, C. L. Guo, J. T. Sheridan, G. H. Situ, M. Naruse, T. Matsumoto, I. Juvells, E. Tajahuerce, J. Lancis, W. Chen, X. D. Chen, P. W. H. Pinkse, A. P. Mosk, and A. Markman, "Roadmap on optical security," *Journal of Optics*, vol. 18, no. 8, pp. 083001, 2016.
- [3] W. Chen, B. Javidil, and X. Chen, "Advances in optical security systems," *Advances in Optics and Photonics*, vol. 6, no. 2, pp. 120-155, 2014.
- [4] S. Liu, C. Guo, and J. T. Sheridan, "A review of optical image encryption techniques," *Optics & Laser Technology*, no. 57, pp. 327-342, 2014.
- [5] S. Jiao, C. Zhou, Y. Shi, W. Zou, and X. Li, "Review on optical image hiding and watermarking techniques," *Optics & Laser Technology*, no. 109, pp. 370-380, 2019.
- [6] P. Refregier, and B. Javidil, "Optical image encryption based on input plane Fourier plane random encoding," *Optics Letters*, vol. 20, no. 7, pp. 767-769, 1995.
- [7] G. Situ, and J. Zhang, "Double random-phase encoding in the Fresnel domain," *Optics Letters*, vol. 29, no. 14, pp. 1584-1586, 2004.
- [8] W. Chen, X. Chen, and C. J. Sheppard, "Optical image encryption based on diffractive imaging," *Optics Letters*, vol. 35, no. 22, pp. 3817-3819, 2010.
- [9] Y. Qin, Q. Gong, and Z. Wang, "Simplified optical image encryption approach using single diffraction pattern in diffractive-imaging-based scheme," *Optics Express*, vol. 22, no. 18, pp. 21790-21799, 2014.
- [10] E. Ahouzi, W. Zamrani, N. Azami, A. Lizana, J. Campos, and M. J. Yzuel, "Optical triple random-phase encryption," *Optical Engineering*, vol. 56, no. 11, pp. 113-114, 2017.
- [11] Z. Liu, L. Xu, Q. Guo, C. Lin, and S. Liu, "Image watermarking by using phase retrieval algorithm in gyrator transform domain," *Optics Communications*, vol. 283, no. 24, pp. 4923-4927, 2010.
- [12] S. Deng, L. Liu, H. Lang, W. Pan, and D. Zhao, "Hiding an image in cascaded Fresnel digital holograms," *Chinese Optics Letters*, vol. 4, no. 5, pp. 268-271, 2006.
- [13] Y. Shi, G. Situ, and J. Zhang, "Optical image hiding in the Fresnel domain," *JOSA A*, vol. 8, no. 6, pp. 569, 2006.
- [14] J.-F. Morizur, L. Nicholls, P. Jian, S. Armstrong, N. Treps, B. Hage, M. Hsu, W. Bowen, J. Janousek, and H.-A. Bachor, "Programmable unitary spatial mode manipulation," *JOSA A*, vol. 27, no. 11, pp. 2524-2531, 2010.
- [15] G. Labroille, B. Denolle, P. Jian, P. Genevaux, N. Treps, and J.-F. Morizur, "Efficient and mode selective spatial mode multiplexer based on multiplane light conversion," *Optics Express*, vol. 22, no. 13, pp. 15599-15607, 2014.

- [16] N. K. Fontaine, R. Ryf, H. Chen, D. Neilson, and J. Carpenter, "Design of high order mode-multiplexers using multiplane light conversion," in European Conference on Optical Communication (ECOC), Gothenburg, Sweden, 2017, pp. 1-3.
- [17] X. Lin, Y. Rivenson, N. T. Yardimci, M. Veli, Y. Luo, M. Jarrahi, and A. Ozcan, "All-optical machine learning using diffractive deep neural networks," *Science*, vol.361, no. 6406, pp. 1004-1008, 2018.
- [18] Y. Shi, G. Situ, and J. Zhang, "Multiple-image hiding in the Fresnel domain," *Optics Letters*, vol.32, no. 13, pp.1914-1916, 2007.
- [19] A. Alfalou, and A. Mansour, "Double random phase encryption scheme to multiplex and simultaneous encode multiple images," *Applied Optics*, vol. 48, no. 31, pp. 5933-5947, 2009.
- [20] B. Deepan, C. Quan, Y. Wang, and C. J. Tay, "Multiple-image encryption by space multiplexing based on compressive sensing and the double-random phase-encoding technique," *Applied Optics*, vol.53, no. 20, pp.4539-4547, 2014.
- [21] X. W. Li, and I. K. Lee, "Modified computational integral imaging-based double image encryption using fractional Fourier transform," *Optics and Lasers in Engineering*, no. 66, pp. 112-121, 2015.
- [22] Q. Wang, Q. Guo, and L. Lei, "Multiple-image encryption system using cascaded phase mask encoding and a modified Gerchberg-Saxton algorithm in gyrator domain," *Optics Communications*, no. 320, pp. 12-21, 2014.
- [23] Q. Wang, A. Alfalou, and C. Brosseau, "New perspectives in face correlation research: a tutorial," *Adv. Opt. Photon.*, no. 9, pp. 1-78, 2017.
- [24] H. Suzuki, M. Yamaguchi, M. Yachida, N. Ohya, H. Tashima, and T. Obi, "Experimental evaluation of fingerprint verification system based on double random phase encoding," *Optics Express*, vol. 14, no. 5, pp.1755-1766, 2006.
- [25] S. Yuan, T. Zhang, X. Zhou, X. Liu, and M. Liu, "An optical authentication system based on encryption technique and multimodal biometrics," *Optics & Laser Technology*, no. 54, pp. 120-127, 2013.
- [26] L.C. Ferri, A. Mayerhoefer, M. Frank, C. Vielhauer, and R. Steinmetz, "Biometric Authentication for ID Cards with Hologram Watermarks. Electronic Imaging," *Security and Watermarking of Multimedia Contents IV*, vol. 4675, pp. 629-640, SPIE, 2002.
- [27] S. Zheng, X. Zeng, S. Xu, and D. Fan, "Orthogonality of Diffractive Deep Neural Networks," *arXiv preprint arXiv:1811.03370*, 2018.
- [28] S. Jiao, W. Zou, and X. Li, "Noise removal for optical holographic encryption from telecommunication engineering perspective," *OSA Digital Holography and Three-Dimensional Imaging 2017*, pp. Th2A-5, Optical Society of America, 2017.
- [29] S. Jiao, Z. Jin, C. Zhou, W. Zou, and X. Li, "Is QR code an optimal data container in optical encryption systems from an error-correction coding perspective?" *JOSA A*, vol. 35, no. 1, pp. A23-A29, 2017.
- [30] <https://github.com/szgy66/code/tree/master>